SAND-77-1185C

HELIOS: A COMPUTATIONAL MODEL FOR SOLAR CONCENTRATORS*

SAND-770850--1

F. Biggs and C. N. Vittitoe
Sandia Laboratories, Albuquerque, New Mexico 87115

ABSTRACT

The HELIOS computer code calculates the power concentrated by a field of individually guided heliostats and the resulting flux density (watts/cm^2) falling upon an arbitrary target grid. The problem has individual subroutines for each task in order to incorporate options for a variety of facet shapes, heliostat designs, field layouts, and tower-receiver apertures, and to facilitate additions and code improvements. HELIOS evolved concurrently with the construction of the Solar Thermal Test Facility (STTF) at Sandia Laboratories and has been used extensively by the STTF engineers to analyze questions on safety, performance, design trade-offs, and tower protection engineering. Comparisons of HELIOS results with measurements have given good agreement.

HELIOS calculates the "sun position" and uses it to establish alignment geometries. Atmospheric attenuation effects are included. Measured angular-distributions of incoming photons (sunshapes) and effects of aureole scattering are incorporated. Nondeterministic factors such as sun-tracking errors and facet-surface errors are described statistically and combined with the sunshape by numerical convolution. Shadowing and blocking are included. Several output choices are available, including graphical display of flux density distributions, of shadowing and blocking and of sunshape.

Some of the modeling in HELIOS and samples of results will be described.

*This work supported by the U.S. Energy Research and Development Administration.

DISCLAIMER

INTRODUCTION

The computer program HELIOS calculates the power concentrated by a field of individually guided heliostats and the flux density (W/cm^2) falling upon an arbitrary target grid. The program evolved over the past two years concurrently with the construction of the Solar Thermal Test Facility (STTF) at Sandia Laboratories in Albuquerque, NM. We worked closely with the STTF engineers and as new questions arose, options were added to the code to answer them and to present the solutions in a convenient form.

It became clear early in the code development that the priority of questions to be answered changed with time. An early priority was performance predictions but soon safety analyses took top priority. Later the emphasis shifted more to design trade-off studies, then to an analysis of calibration and alignment effects and to general parameter studies. This required us to adopt a philosophy of constructing a usable computer program quickly using approximations where necessary, then to improve upon them as the needs were identified. Moreover, it was necessary to structure the program with individual subroutines for each major task to facilitate the addition of new options for an everchanging variety of facet shapes, heliostat designs, field layouts, and target-grid specifications.

As HELIOS continued to evolve, there were fewer new kinds of questions to answer and the emphasis shifted from adding new capabilities to improving existing ones, streamlining the code, and documentation work. We are still in the latter phases of the project. A users guide is now available (Ref. 1) and a report giving the development of the model is in progress (Ref. 2). Preliminary versions of HELIOS have now been distributed to several agencies outside Sandia Laboratories.

The remainder of this report is organized as follows: (1) an overview summarizes the important functions of the model, (2) some of the statistical optics are examined, (3) a more detailed description of the computer code is given emphasizing the input parameters, and finally (4) some examples of auxiliary programs are presented.

MODEL DESCRIPTION

Figure 1 shows a schematic drawing of a central-receiver solar-collector system emphasizing the important elements. Three heliostats are shown on a small hill to illustrate that the ground may not be level. There are, of course, more than three heliostats in the usual collector field but these will be adequate to illustrate

the main ideas of the model including shadowing and blocking.

From the time a photon leaves the sun until it reaches the receiver aperture, it is subjected to many effects. HELIOS is designed to simulate these effects and to determine the consequences of them on the performance of the collector system. We now give an overview of the model organizing the discussion in roughly the order a photon encounters the system.

We first go through the system to define a few special terms, then go back through it describing effects and how HELIOS simulates these effects. The "central ray" from the sun originates from the center of the solar disk. The "sun position" is the direction (azimuth and elevation) of the incoming central ray. Each heliostat consists of one or more reflecting surfaces called "facets". Figure 1 shows 9 facets for convenience in drawing. The heliostat is guided so that a central ray from the sun will reflect from the center of the "reference facet" (center facet) to intersect the "aim point". The distance from a heliostat reference-facet to the aim point is called the "slant range" for that heliostat and the path followed by a reflected central ray is called the "slant-path". The facets also have slant-ranges, these may differ slightly from the corresponding heliostat slant-range. The "target-grid" is a grid of points at which HELIOS calculates the "flux density" in watts per cm^2.

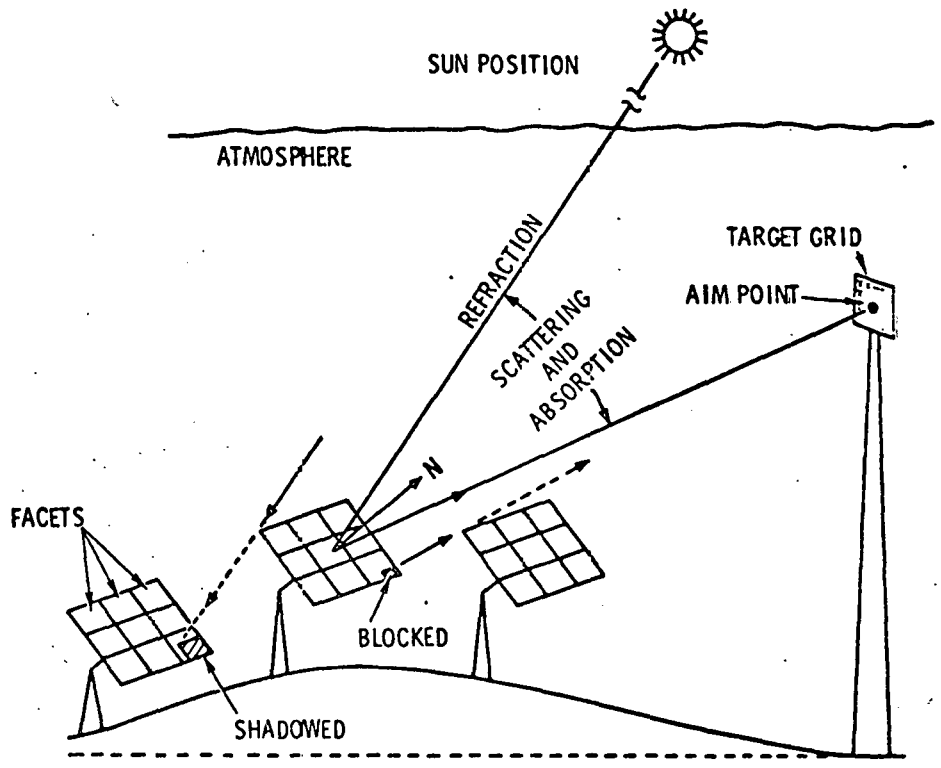

Figure 1. A schematic drawing of a central-receiver solar-collector system showing a three-heliostat portion of the collector field.

The central ray does not follow a straight path through the atmosphere but is curved by refraction. HELIOS

determines the sun position (actually apparent sun position) that corrects for atmospheric refraction. This information is subsequently used by the code to help establish alignment geometries for the heliostats.

Photons are incident on the atmosphere, not as a collimated beam of light but with an angular distribution of directions, called the "sunshape", about the central ray. The solar disk subtends an angle of approximately 10 mrad as viewed from the earth. As sunlight traverses the atmosphere scattering (aureole scattering) broadens the sunshape. This is especially evident during hazy atmospheric conditions. HELIOS uses sunshapes that are measured at the collector site.

As sunlight traverses the atmosphere, it is attenuated by absorption and scattering. Several models of the atmosphere are available to determine insolation at the site and to calculate absorption losses along the slant paths from each heliostat to the tower receiver. Measured values of solar insolation can also be used as input.

Each heliostat is aligned by rotation about two axes. The alignment is calculated so that the central ray reflecting from the center of the reference facet (center facet) will intercept the aim point. Since the alignment rotations may cause displacements of the reflecting surface, the alignment calculation is iterated until the calculation is based on the correct final position of the reflecting surface.

The facets are prealigned with respect to the heliostat frame to obtain the desired focal properties for the heliostat. Figure 1 shows 9 facets per heliostat for simplicity in drawing; however, zone-A heliostats of the STTF have 25 facets. It is, of course, possible to have only one facet per heliostat. A common "prealignment" option is designated as "on axis" where the facets are set so that light incident and reflected at a zero angle of incidence would come to a focus at a distance from the heliostat equal to its slant range. In this option, the total heliostat surface approximates a paraboloid of revolution as closely as is possible by the prealignment of facets. Another option is obtained by specifying a date and time of day from which HELIOS calculates an apparent sun position and then uses it to determine the prealignment conditions that will permit central rays to reflect from the center of each facet to intercept the aim point at the specified time. The prealignment information is stored and used in subsequent calculations.

Several options are available for specifying facet shapes, among these are flat, spherical, paraboloidal, and some surface shapes obtained from stress-analysis calculations. If the shape is specified to be paraboloidal, a focal length equal to the slant range is used. In the present stress-analysis options a facet center pull-down distance is used to adjust the focal properties of the facet. HELIOS uses an optimization routine to find the value of the pull-down parameter that maximizes the flux density in the solar image projected on the target grid for each facet.

As shown schematically in Figure 1, a heliostat may be partially shadowed from the sun by another heliostat or a heliostat may block light that is reflected from another one. These effects are calculated by HELIOS and options are available to display the results graphically.

The aim point is used for heliostat guidance calculations. It would usually be placed at the center of the receiver aperture for most performance calculations, but it would be someplace else for purposes of simulating a standby mode of operation. Separate aim points for different heliostats can be specified if desired. This would be necessary for some shapes of receiver apertures. Aim points are also used in the prealignment calculations but these are specified separately from those used in the simulation "run-time" calculations. The run time consists of a date and time of day which is used by HELIOS to calculate the corresponding apparent sun position which it then uses to determine the heliostat alignment geometry.

The target grid is shown in Figure 1 to coincide with the receiver aperture and centered on the aim point. Although this is a common arrangement for performance calculations, the specification of the target grid is independent of the aim point; it can be placed anywhere. It may be positioned on the tower to simulate spillage effects in order to answer questions on tower-protection engineering. The target grid is shown as rectangular in Figure 1, but options are available for it to be spherical, cylindrical, or an arbitrary shape to be specified by the user. Currently, the code is set up to calculate the flux density (W/cm^2) at 121 points (on an 11 by 11 grid) on the target grid. It also calculates the radiant power obtained by integrating over the target grid.

When the computer calculates heliostat alignments, it does so to machine accuracy whereas the sun-tracking mechanism can guide the heliostats to within some (much more course) error tolerance. A similar effect occurs

in the prealignment of facets. There are also many other nondeterministic factors that degrade the performance of the system. The facet shapes vary about their designed shapes because of manufacturing tolerances, because of temperature effects, and even because of changes in gravity loading as the heliostat tracks the sun. Turbulent wind-loading may cause the facets to vibrate. There is a non-specular component to the reflection of sun light. These nondeterministic factors degrade the average performance of the solar collector. It is important to include them in a model that simulates the behavior of the system.

HELIOS subdivides each facet into an integration mesh. It then calculates a contribution to the flux density at each of the target grid points from one of these integration-mesh areas. The program then cycles over the integration mesh of the facet to obtain the facet contribution. It cycles over the facets of the heliostat and finally over the heliostats of the field.

Figure 2 shows one block of the integration mesh within a facet. The incident central-ray from the sun lies along vector I. The cone drawn about I depicts the angular distribution of incoming sun rays (sunshape). The vector N shows the nominal direction of the normal for this element of surface and the cone drawn about N

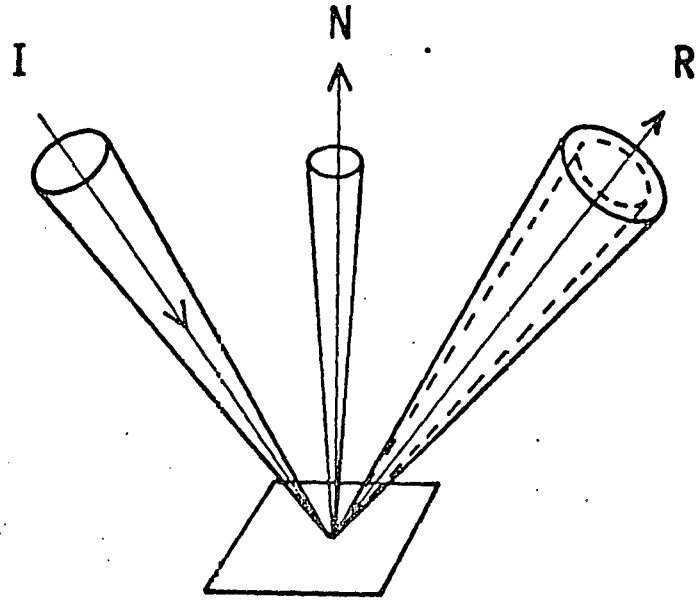

Figure 2. The broadening of the effective sunshape due to uncertainty in the direction of the reflecting-surface normal.

depicts the nondeterministic nature of the direction of this surface-normal due to the uncertainties mentioned above. If the surface normal were known to lie along N (no uncertainty) then the reflected sunshape would be as shown by the dotted cone about the reflected central ray R. With uncertainties in the direction of the surface normal, the reflected cone is spread out (on the average) as indicated by the solid cone drawn about R. We call this the "effective sunshape". The effective sunshape is projected onto the target grid to obtain the average contributions to the flux density at each

of the target-grid points.

The distribution of directions of the surface normal is mapped into a distribution of directions of reflected rays about R and combined numerically with the reflected sunshape using the two-dimensional fast Fourier transform to obtain the effective sunshape. This characterizes the distribution of reflected sun-rays when averaged over time and reflecting surface.

AN ILLUSTRATION

As an illustration of the use of HELIOS, we examine the flux-density pattern on the Martin Marietta one Megawatt Receiver that is produced by the 78 heliostats of zone A of the STTF. We also analyze some of the factors that cause this flux-density pattern to change with time.

The shadowing projection of Figure 3 is convenient for showing the heliostat arrangement. The 78 heliostats and the tower are projected onto a plane through the base of the tower and perpendicular to the central ray from the sun at noon on March 21. This is, therefore, a veiw of the collector field and tower from the south at an elevation of 55 degrees.

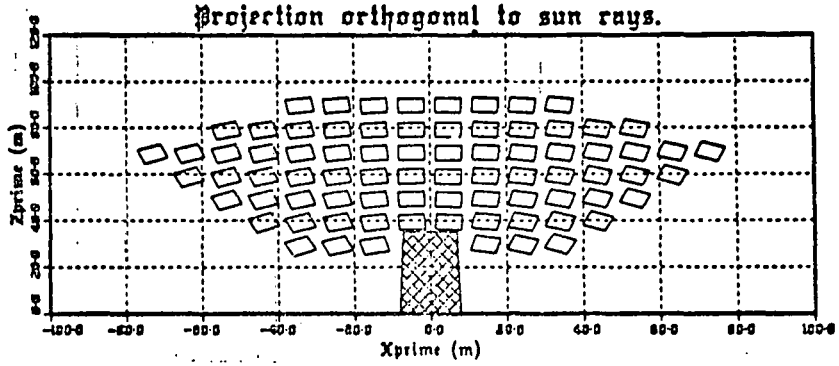

Figure 3. The tower and 78 heliostats of zone A of the STTF. This is a projection on a plane through the base of the tower and perpendicular to the central ray from the sun at noon on March 21. The xprime axis is horizontal.

The 1-m by 1-m receiver aperture on the tower faces north, it is centered at an altitude of 44.5 m above the base of the tower, and is inclined downward 20° from the vertical. The prealignment of facets is for noon of March 21. This means that the facets are prealigned with respect to the heliostat frame so that central rays from the sun reflect from the center of each facet to intercept the aim point while in the geometry of Figure 3, i.e., at noon on March 21. We assume an insolation of 800 W/m^2 and a facet reflectivity of 0.8 for this example.

Figure 4 shows the sunshape (dotted curve), the error cone (dashed curve), and the resultant effective sunshape (solid curve). A circular-normal error-cone of

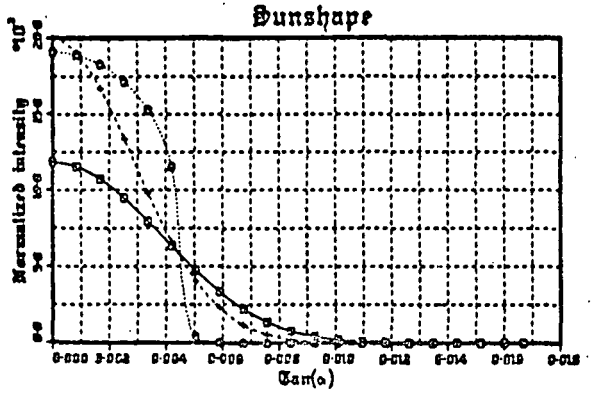

Figure 4. The sunshape (dotted curve), the error cone (dashed curve) and the effective sunshape (solid curve).

dispersion equal to 2 milliradians is used. The sunshape is one that was measured in Albuquerque, NM at 1 PM on June 25, 1976.

Figure 5 shows flux density (W/cm^2) patterns on the receiver aperture. Part a corresponds to 8 AM and part b to noon; both are for March 21. The peak flux density at noon is about 300 watts/cm^2 (3750 suns) and the integral of the flux density over the 1-m by 1-m aperture is 1.36 MW which corresponds to 1700 suns when averaged over the aperture. Thus the average flux density is a little less than half the peak value. At 8 AM (part a) the peak value of the flux density is about 120 watts/cm^2 (1500 suns) and the power intercepted by the aperture is 0.66 MW. This gives an

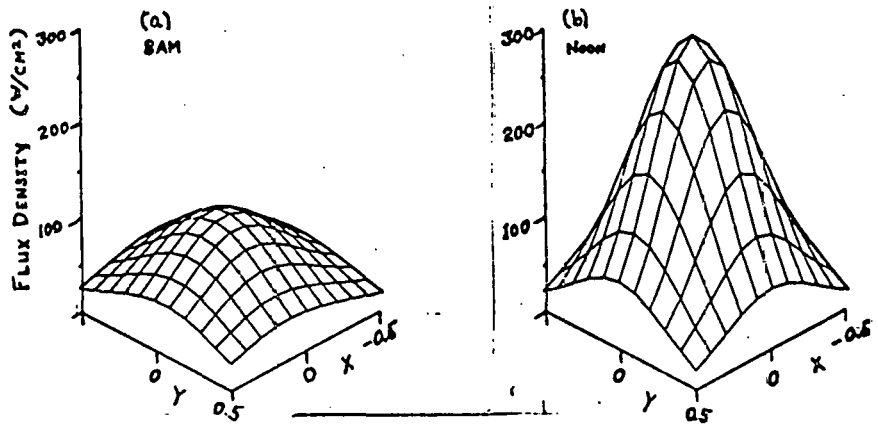

Figure 5. Flux-density patterns on the 1-m tower receiver aperture from the 78 heliostats of zone A of the STTF on March 21. The prealign time is noon of March 21.

average of 66 Watts/cm^2 (825 suns) over the aperture which is a little more than half the peak value. There is, therefore, a significant flattening out of the flux density pattern between the noon and the 8 AM results.

Let us take a more detailed look at the reasons for the differences between these two flux density patterns. The total collector area for the zone A field is $A = (1.22)^2(25)(78) = 2902\ m^2$. If this area were normal to the central ray from the sun, it would intercept a power of $P = AQ = (2902\ m^2)(800 W/m^2) = 2.32$ MW where $Q = 800\ W/m^2$ is the insolation. Of course, the area A is not all perpendicular to the sun's rays but

is effectively reduced by the "cosine effect". Shadowing and blocking together with other factors also contribute to losses in the power collected. It is of interest to use results from HELIOS to compare the loss factors corresponding to the two flux-density patterns of Figure 5.

The first row of Table 1 gives the cosine-effect loss factors for the two run-times. The number in parenthesis in the 8 AM column is the ratio of the 8 AM value to the corresponding noon-time value. Thus the cosine-effect loss-factor at 8 AM is 88% of its value at noon. The reflected power (neglecting shadowing and blocking) is given in the next row. This is the product of the total collector area A = 2902 m^2, times the insolation (800 W/m^2), times the reflectivity $\rho = 0.8$, times the cosine-effect loss-factor from the first row. The next row gives the shadowing and blocking loss factors, multiplying these by the numbers in the row above gives the effective reflected power. However, not all the effective reflected power is intercepted by the receiver-aperture. There is a spillage loss-factor which is given in the next to the last row of the table. At 8 AM, only 49% of the effective reflected power intercepts the aperture to give a collected power of 0.66 MW. At noon, 80% of the effective reflected power intercepts the aperture giving a collected power of 1.36 MW.

Table 1 - Loss factors for performance of the 78 heliostats of zone A of the STTF with the 1-m by 1-m Martin Marietta 1 MW receiver and using a circular-normal error-cone of dispersion equal to 2 milliradians. Pre-alignment time is noon of March 21. The run times listed below are also for March 21. The facet reflectivity is $\rho = 0.8$ and $P = (2902\ m^2)\ (800\ W/m^2) = 2.32$ MW. The numbers given in parenthesis in the 8 AM column are ratios of the loss factor at 8 AM to its value at noon.

	Run Times	
	8 AM	Noon
Cosine-effect loss-factor = $< \cos i >$	0.84 (0.88)	0.96
Reflected power neglecting shadowing and blocking loses = $P\rho < \cos i >$	1.56 MW	1.78 MW
Shadowing and blocking loss-factor	0.87 (0.91)	0.96
Effective reflected power	1.36 MW	1.71 MW
Spillage loss-factor	0.49 (0.61)	0.80
Collected power	0.66 MW	1.36 MW

Note that the loss factor that changes most between the noon and 8 AM run-times is the spillage loss-factor (the smallest of the numbers in parenthesis of the 8 AM column). In order to illustrate how heliostat-size astigmatic-aberrations contribute to the spillage loss factor, we use some more HELIOS results.

Consider the flux-density patterns resulting from only the four corner facets of heliostat #18 of the zone A field. This heliostat is in the bottom row of heliostats shown in Figure 3 and just to the left of the shadow of the tower. Figure 6 shows the flux density pattern in part a for a run time of 11 AM and in part b for a run time of 3 PM. The prealignment of facets and the run times in this example are different from those used in the previous results but the concepts to be illustrated are the same. These four facets are assumed to be aligned on-axis (zero angle of incidence). This is approximately the situation in part a of Figure 6 where the angle of incidence is only 3 degrees. The target grid is centered on the Martin Marietta one-Megawatt receiver-aperture but we have enlarged it to 2.5-m in order to show more of the spillage pattern and to better illustrate the effect of astigmatic aberrations. The 1-m by 1-m receiver aperture would occupy a 4-block by 4-block square in the center of the target grid shown in the figure.

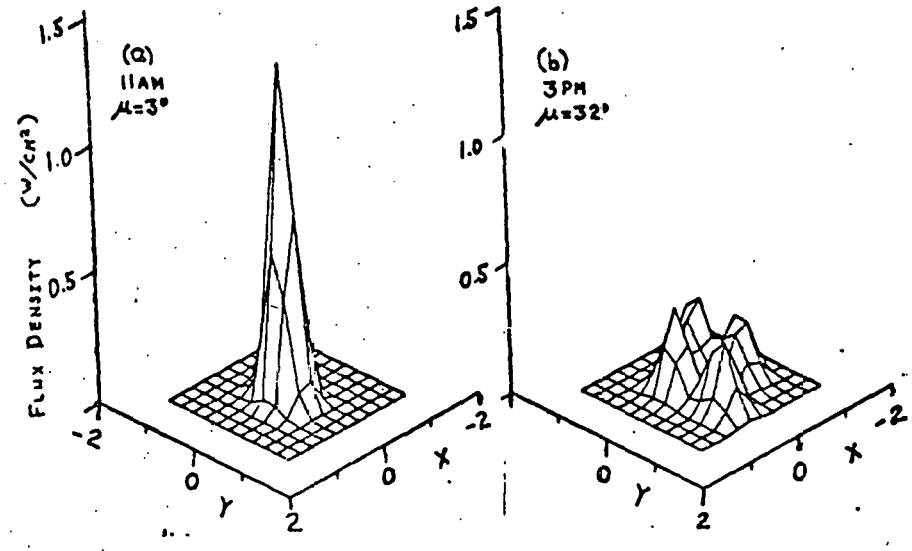

Figure 6. Flux-density patterns from the four corner facets of heliostat #18. In part a, the run time is 11 AM on March 21 and in part b the run time is 3 PM on March 21. The facets are prealigned on-axis.

The heliostat alignment in both parts of Figure 6 is such that the center facet would project a solar image centered on the aim point (the center of the target grid here). If all the facets of the heliostat were used in the calculation, the flux-density pattern in part a of Figure 6 would be similar in shape but more intense by a factor of about 25/4 = 6.25. In part b, however, the individual peaks would no longer be resolved but a generally smeared out pattern would be obtained.

This illustrates the major reason for the change in the spillage loss-factors between the a and b parts of Figure 5. Of course, in Figure 5, the flux patterns are for the 78 heliostats of zone A of the field. The extent of the astigmatic aberrations changes from one heliostat to another because of the different geometric relationships between each heliostat and its prealignment conditions. HELIOS is designed to facilitate such parameter studies as these.

CODE ORGANIZATION AND INPUT CAPABILITY

In keeping with the conference objective of providing a description of the computer code for specialists and potential users, we now concentrate upon the code input as a means of further indicating the capabilities of HELIOS. The discussion should convince you that use of HELIOS is easy and is reasonable for many types of problems.

The basic flow chart is given in Figure 7. The LOCK and NTLOCK parameters allow calculation of the energy flux pattern in two emergency situations, (1) the sun continues across the sky after motors have been locked by a power failure, or (2) the sun continues across the sky after an emergency caused the motors to slew toward the storage position.

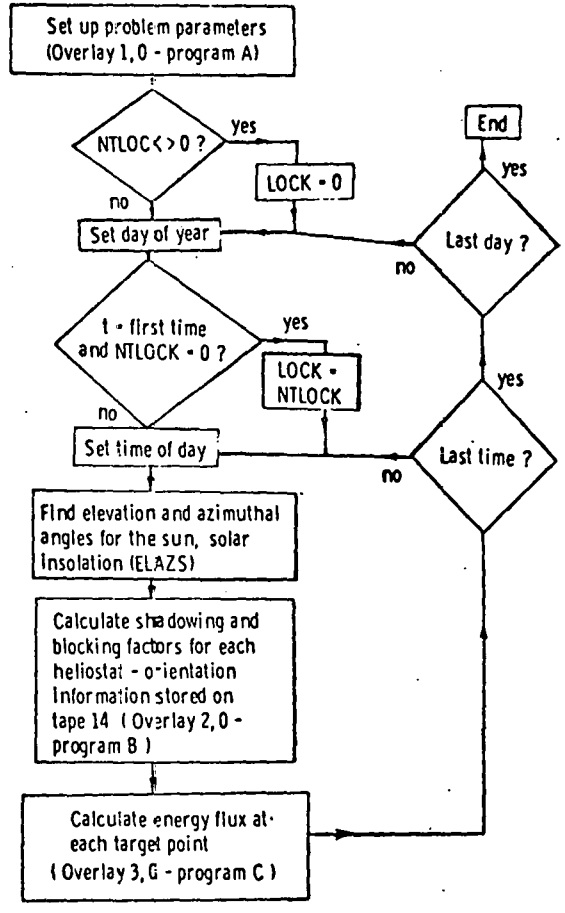

Figure 7. HELIOS Flow Chart

Program A is further subdivided in Figure 8 where controlling subroutines are identified by parenthesis. DATA1 sets the default values appropriate for the Solar Thermal Test Facility at Sandia Laboratories. INDATA accepts all the input variables. This subroutine should be studied by prospective users to increase

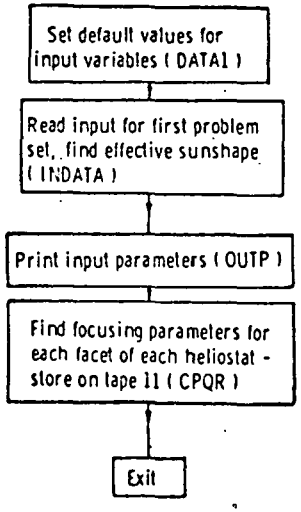

Figure 8. Program A Flow Chart

understanding of code capabilities and to identify possible errors in input data.

The HELIOS input data are separated into seven groups: problem- and output-type data, sun-parameter data, receiver data, facet data, heliostat-positioning data, time data, and atmospheric data. Each set is characterized by a group number NGRUP. As each new problem is encountered, new data need only be read in for groups with data differing from the previous problem. Hence, each set of data may be discussed separately from the other groups. Each of the data groups is now examined briefly with mention of decisions to be made for each group.

Figure 9 gives the group 1 input. Do you want print out for each facet, or for each heliostat, or only for the heliostat field? Are graphs to be generated? Which shadowing and blocking options are to be used? Do you want rapid calculation with less accuracy or improved accuracy with extended computer time? Is a new heliostat distribution to be input or is the STTF default distribution sufficient? Is the propagation loss between mirror and receiver to be included?

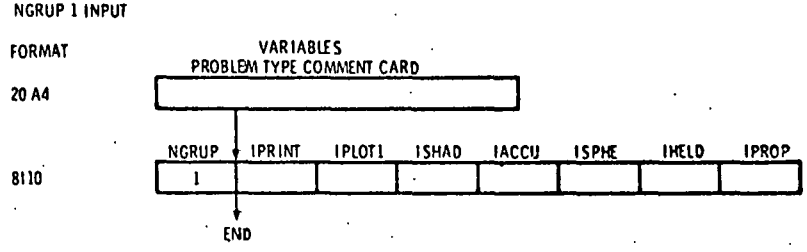

Figure 9. Group 1 input flow chart.

Group 2 data control the effective sunshape. The parameters in Figure 10 determine the sunshape, error cone, and effective sunshape. They also allow solar insolation as an input variable. The sunshape may be inserted via parameters or as a table of values.

The receiver data are input as group 3 in Figure 11. They specify the number of target points, printing options, target orientation, target shape, receiver latitude, coordinates of the target center, of the

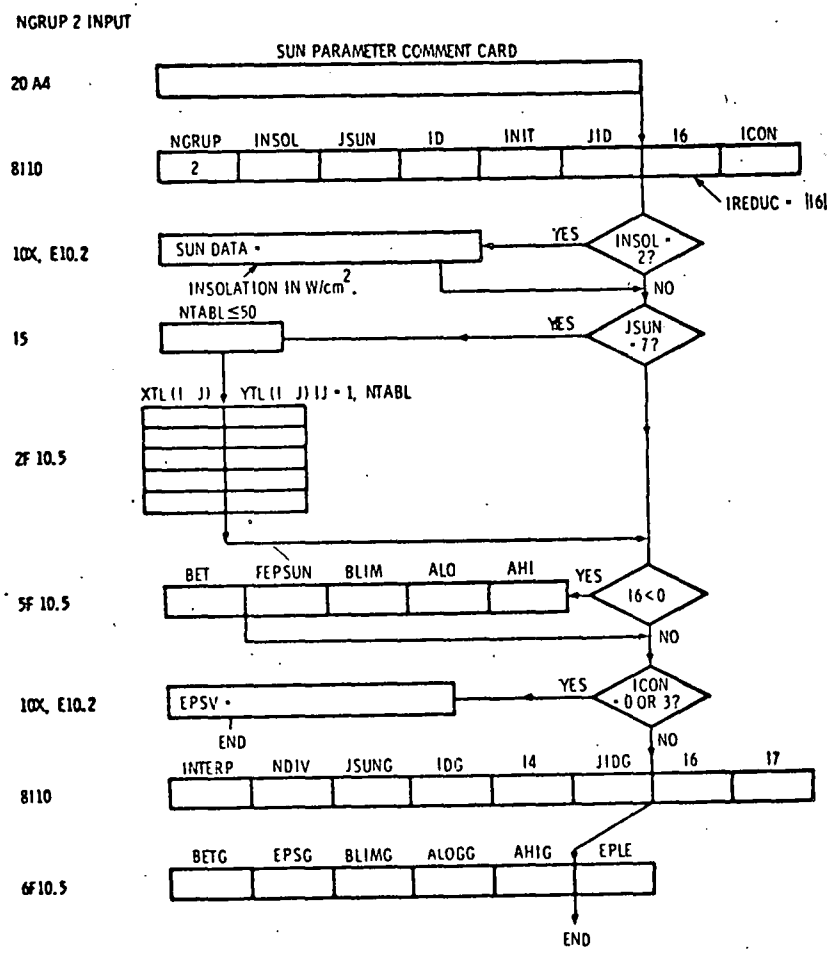

Figure 10. Group 2 input flow chart.

aim point, and of the prealignment point, and effective tower dimensions for shadowing calculations.

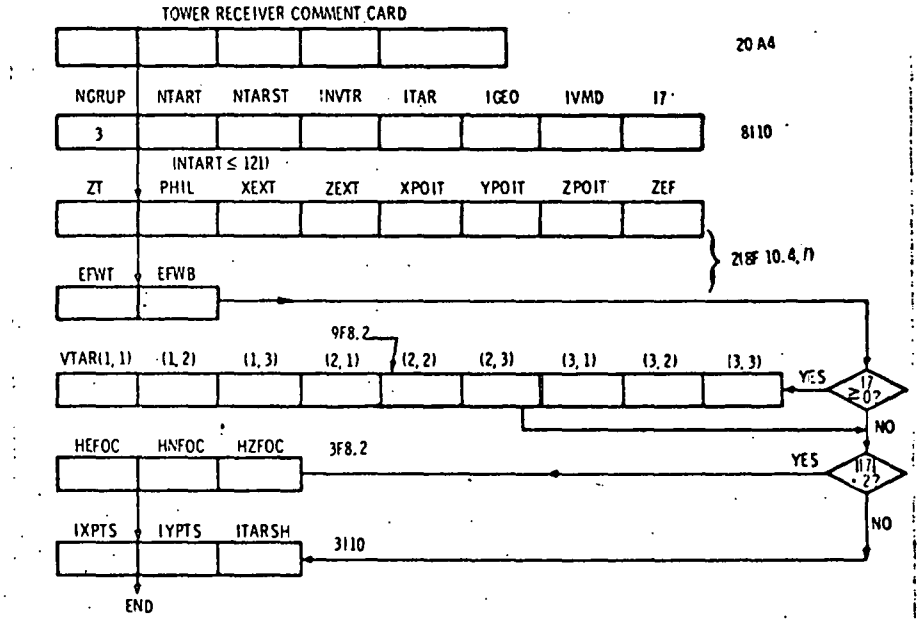

Figure 11. Group 3 input flow chart.

Figure 12 gives the flow chart for the facet data. How many facets are on each heliostat? Are the facets circular or square? How many subdivisions of the facet are to be taken along each edge? What is the surface shape? If a shape resulting from stress analysis is to be used, what is the radius of a stressed ring or disk, and what is Poisson's ratio for the stressed material? What is the facet dimension? Reflectivity? Distribution on the heliostat?

The facet distribution on the heliostat is given in Figure 13. The U3 axis completes the right handed coordinate system. The coordinate of the facet centers

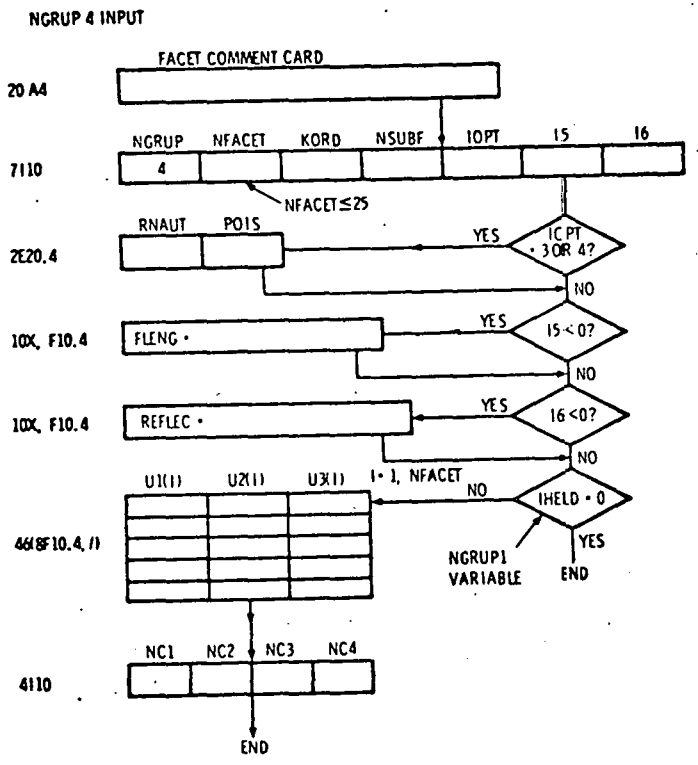

Figure 12. Group 4 input flow chart.

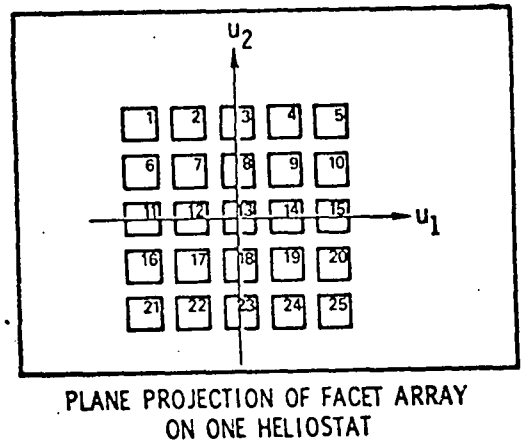

Figure 13.

are needed to properly locate each facet in space.

Heliostat parameters are furnished by the group 5 data in Figure 14. Heliostat identifying numbers, the number of heliostats to be treated, the prealignment strategy, and the emergency parameters are all input here. If a new heliostat distribution is to be input, its x, y, z coordinates are read here along with heliostat design parameters. These variables are shown in Figures 15-16.

The time-data input for group 6 are shown in Figure 17. Here the calculation times and prealignment time are specified.

Group 7 of the input gives the atmospheric data. The variables in Figure 18 specify the model atmosphere to be used when solar insolation is to be calculated. The pressure and temperature variables also have a slight effect on the solar refraction.

The appendix describes general program characteristics, limitations, running time, hardware and software requirements. An early version of the users manual is also available for greater detail (Ref. 1). Let us assume you are now convinced that HELIOS is easy to use. Is it reasonable to use? What real tests of the code are available for checking code accuracy?

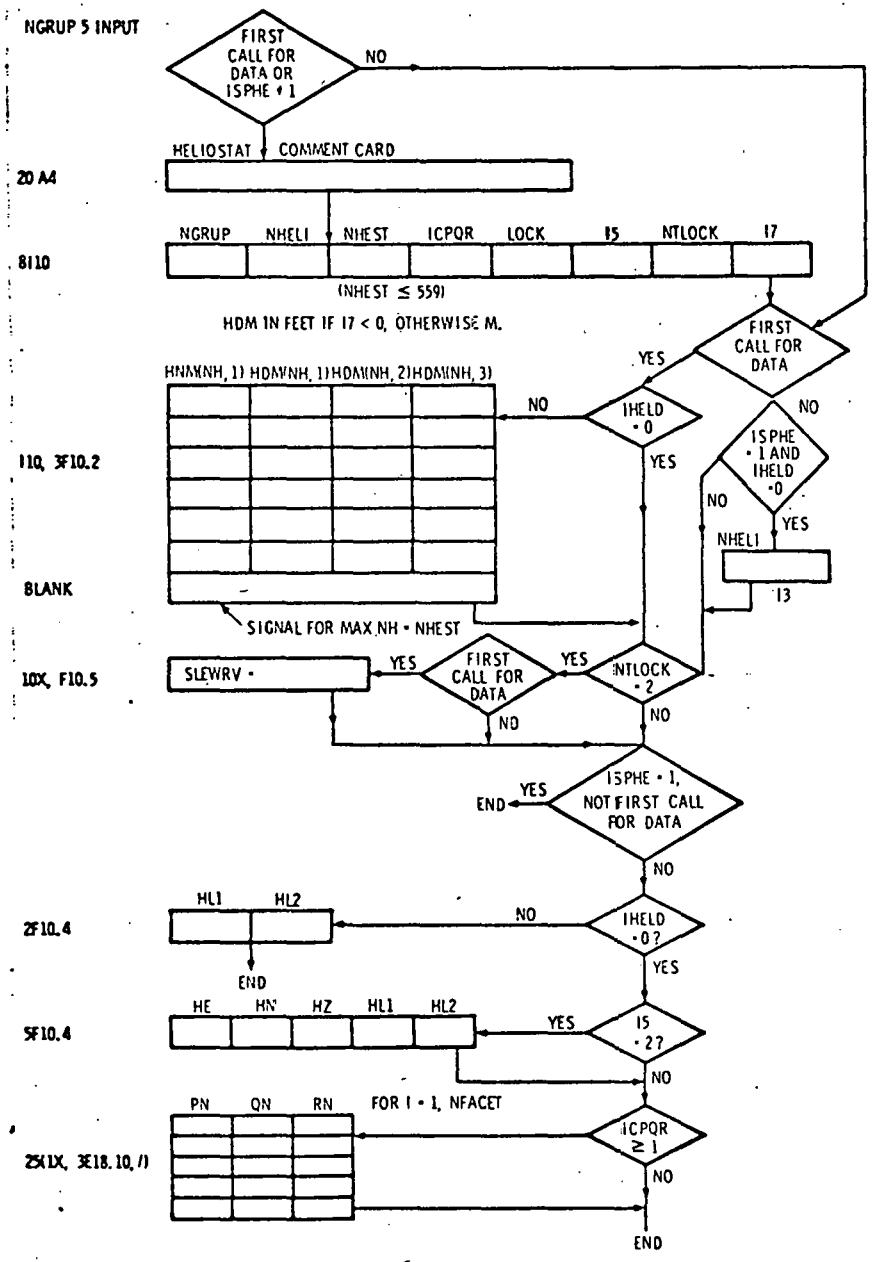

Figure 14. Group 5 input flow chart.

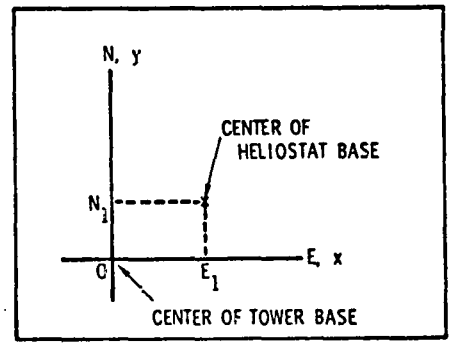

HELIOSTAT DEPLOYMENT IN TOWER COORDINATE SYSTEM

Figure 15. Heliostat deployment in Tower Coordinate System. x = HDM(NH,1), y = HDM(NH,2), z = HDM(NH,3).

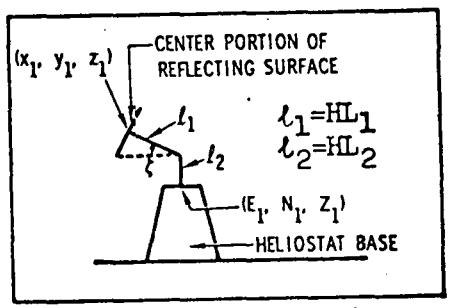

SAMPLE HELIOSTAT MOUNTING

Figure 16. Sample heliostat mounting.

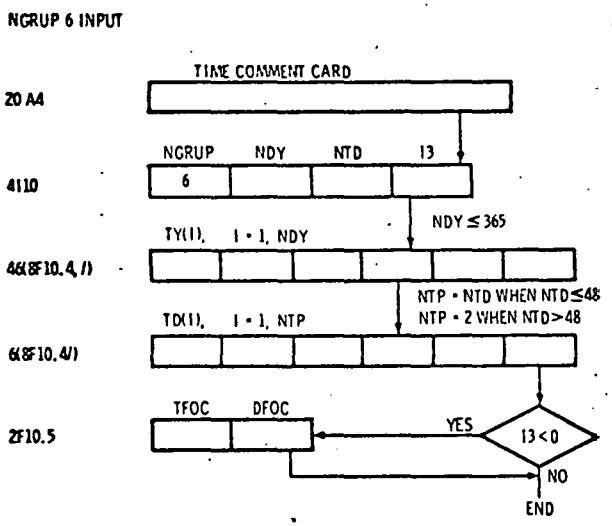

Figure 17.

Group 6 input flow chart.

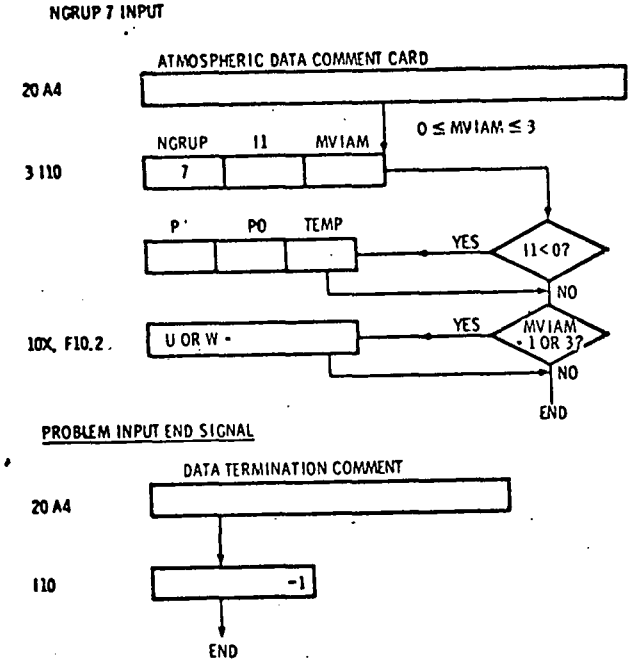

Figure 18.

Group 7 input flow chart and end signal.

HELIOS CHECKS

Figure 19 summarizes the checks of HELIOS to date. Several verifications of the shape of the intensity pattern for a single mirror were made by Larryl Matthews. Shapes were checked near the saggital and tangential focal planes. Shape checks were also made for a few facets on a single heliostat in scale model experiments (Ref. 3). The shape of the energy flux pattern for a field of heliostats was verified by John Holmes.

CHECK POINTS FOR HELIOS

1. Scale model experiments for one heliostat by E. A. Igel, G. F. Bott, R. L. Hughes, April 1977.
2. MIRVAL computer code comparisons by J. D. Hankins ~ January 1977.
3. Comparisons with shape of hole in iron plate by John Holmes ~ May 1977.
4. Shape comparisons with image formed by 80' focal length spherical mirror by Larryl Matthews ~ April 1976.
5. Comparisons with Martin-Marietta data for one facet by W. Hart and C. N. Vittitoe ~ April 1977.

Future:

1. Comparison with measurements at Georgia Institute of Technology by B. G. Levi.
2. Comparison with measurements at the Solar Thermal Test Facility with concurrent measurement of incident sunshape.

Figure 19. Check points for HELIOS.

Magnitude and shape comparisons for the energy flux from one heliostat were reported by Joe Hankins to be consistent with his MIRVAL code. Magnitude and shape comparisons have also been made with experimental data collected by Martin Marietta for one facet. These data are given in Figures 20-21. Uncertainty in the sunshape and in the time of data collection suggest the agreement can be improved with more complete information. The sunshape used in the calculation is given in Figure 4. A larger error cone should improve the consistency shown here.

THE SHADOWING AND BLOCKING

One of the HELIOS options which is sometimes useful is the computer drawn plots indicating the extent of shadowing and blocking. The shadowing is illustrated by projecting the corners of each heliostat onto a plane through the tower base, orthogonal to the sun's central ray. An example was given in Figure 3. The blocking is given in Figure 22 as the projection of the corners of each heliostat onto a unit sphere with its origin at the center of the target aperture. The bar graphs at the bottom-left indicate the effective facet area (m^2) before and after shadowing and blocking. Other bar graphs give the power intercepted by the heliostats and the power incident upon the target aperture (in units of 10^5 W).

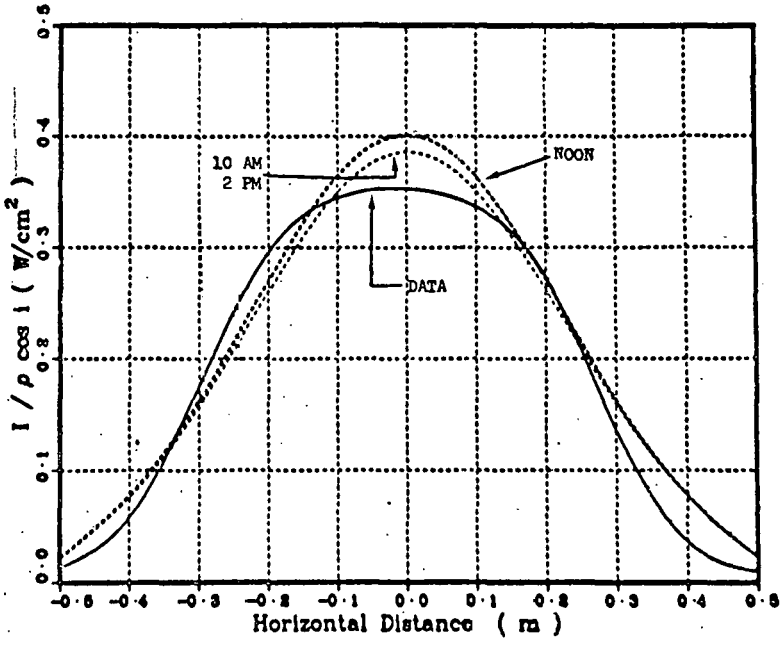

Target is 56.4 m along a line 34° to the east of south of the facet. Insolation is normalized to 0.08 W/cm². Latitude is 39.8° N as for Denver, Colorado. Target and facet heights are identical. The distance is horizontal distance across the target center. The planar target faces the facet.

Figure 20. Energy flux comparison with Martin Marietta data collected on November 23, 1976.

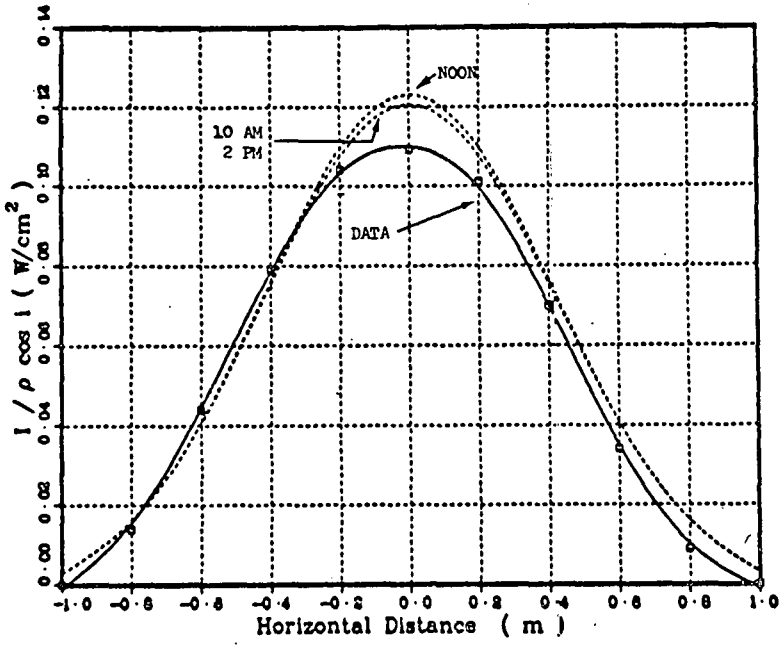

Target is 106.68 m along a line 34° to the east of south of the facet. Insolation is normalized to 0.08 W/cm². Latitude is 39.8° N as for Denver, Colorado. Target and facet heights are identical. The distance is horizontal distance across the target center. The planar target faces the facet.

Figure 21. Energy flux comparison with Martin Marietta data collected on September 28, 1976.

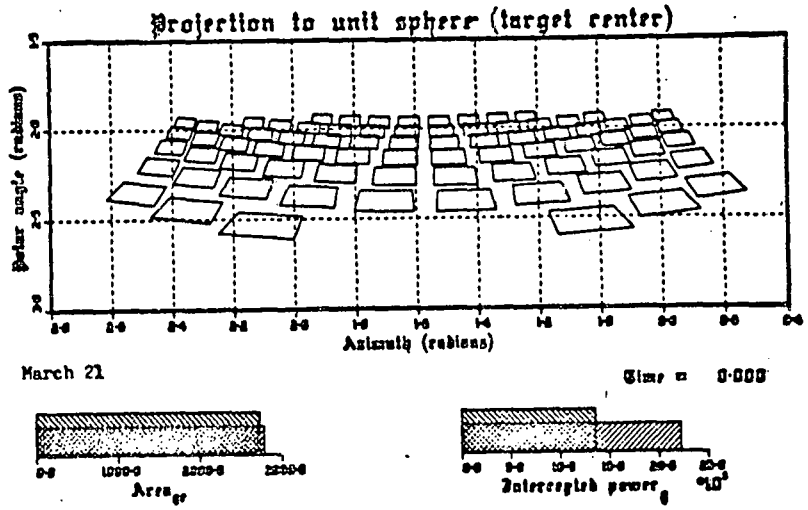

Figure 22. Blocking diagram.

ACKNOWLEDGEMENT

HELIOS has benefited from interactions with many individuals. Much of its flexibility resulted from discussions with J. T. Holmes, D. J. Kuehl, and L. K. Matthews of Sandia Laboratories. Extension to new heliostat deployments resulted from contact with B. G. Levi of Georgia Tech and with W. Hart and J. Williamson of Martin-Marietta. C. S. Hoyle of SLL furnished the subroutine giving the facet-shape that results from stress analysis. P. Van Delinder and W. C. Burd at SLA provided guidance through the early plotting pitfalls. Further benefits are expected from interactions at this workshop.

APPENDIX 1. HELIOS CODE SUMMARY

HELIOS purpose: The code was developed to evaluate proposed designs for central receiver solar energy collector systems, to perform safety calculations on the threat to personnel and to the facility itself, to determine how various input parameters alter the power collected, and to evaluate possible design trade-offs.

HELIOS structure: The code is designed with numerous subroutines for treating individual effects. This structure facilitates additions that have been necessary as special requirements appeared or as improvements became necessary. The additions also resulted in non-optimum code design which will likely remain for some time as effort remains concentrated upon additional options.

Mathematical method: The method for evaluating flux density is basically the cone-optics approach. Reflector surfaces are divided into small segments that are treated as infinitesimal mirrors that reflect a solar image onto the target surface.

HELIOS input: Input variables include atmospheric variables; sunshape parameters; coordinates for heliostat bases relative to the tower; heliostat design parameters, reflector shape information; data describing the uncertainty resulting from surface errors, suntracking errors, non-spectral reflection, and wind loading; focusing and alignment strategy; aim point coordinates; receiver design; calculation time; parameters indicating effects to be included; and the chosen output options.

HELIOS output: Three output options are available. The first gives the flux density (W/cm^2) produced by all the heliostats at the grid of target points. The power intercepted by the mirrors and that incident upon the target are given. The facet area reduced by the angle of incidence effect and the area further reduced by shadowing and blocking effects are given. These data are given for each designated calculation time.

The second output option yields the above output variables for each heliostat in addition to the total. The loss factor caused by light propagation between facet and receiver is also given for each heliostat.

The third output option is still more complex. It is especially useful for detailed examination of results for checking prior to a large computer run. It includes facet and heliostat alignment information, sun orientation, target point alignment information, and detailed shadowing and blocking information including lists of the blocked (shadowed) and blocking (shadowing) heliostats.

All the output options include (1) a table describing the built-in model of atmospheric mass as a function of apparent elevation angle of the sun, (2) a table describing the built-in model of atmospheric refraction as a function of solar elevation angle, (3) brief descriptions of the input data groups, (4) tabular distributions of the sunshape, the error cone, and the effective sunshape, (5) tower coordinates of each target point and the components of the unit vector normal to the target surface at each point in the grid, and (6) a listing of the main problem parameters. As a special output option, the three components of the energy flux density are available at each target point in the grid.

Present HELIOS limitations:

$1 \leq$ number of heliostats ≤ 559
$1 \leq$ number of facets/heliostat ≤ 25
$1 \leq$ number of target points ≤ 121

RELATED CODES:

BLOSH - movie generation for shadowing and blocking
CDC-7600 15 s/frame for plot tape generation for moderate shadowing and blocking. About 50 s/frame for 222 heliostats in zones A-B of the Solar Thermal Test Facility for 4-5 PM on December 21.

CDC-6600 7 s/frame for post processing to obtain tape for microfiche generation of the DX4460 microfilm system.

PLO - plotting program for flux density distribution, shadowing and blocking diagrams, sunshape distribution, etc.

Running time: The required running time is highly dependent upon input options. It is dominated by the flux density calculation except at very late or early times when shadowing and blocking may be extensive. On CDC-7600 with perfect-focus option, the flux density calculation requires ~ 14.4 ms per facet for 121 target points. Zones A-B and A-C-D-E (222 heliostats) of the Solar Thermal Test Facility require 11 to 18 s for shadowing and blocking calculations as those effects reduce the effective mirror area by factors 0.99 to 0.81. Typical CDC 7600 run time for

222 heliostats with 25 facets/heliostat and 121 target points is 120 s including generation of the plot tape. These times should be multiplied by $\leq n^2$ if the facets are divided into a n x n mesh for more precise integration.

Computer hardware requirements: HELIOS is operational on the Sandia Laboratories CDC 6600 computer operating under Scope 3.3. The code requires 142,000 octal storage which may be reduced to 77,000 octal locations after the few seconds required for effective sunshape calculation. HELIOS is also operational on the Sandia Laboratories CDC 7600 under Scope 2.1.

Some auxiliary equipment are necessary. Printer - required; microfiche output - useful; punch - necessary for some options; auxiliary storage - necessary for recall of data temporarily on magnetic tape (disk).

Computer software requirements: The coding language is FORTRAN extended - version 4. Required subroutines from the Sandia Laboratories library that are not distributed by the computer manufacturer are:

FOURT - fast Fourier Transform

MINA - find minimum of a function

QNC7 - integration routine with checking routines ERRCHK, ONECHK, ERRPRT, ERXSET, and ERRGET.

SAXB - solve system of real linear algebraic equations with checking routines RFBS, RULD, and ERSTGT.

These routines are included on HELIOS program tapes. The routines are mentioned in the following reference.

R. E. Jones and C. B. Bailey, Brief Instructions for Using MATHLIB (Version 6.0), Sandia Laboratories Report SAND-75-0545, February 1976.

For CDC 6600 use, one other supplementary routine is available. The REDUCE subroutine allows reduction of the core storage by deletion of blank common that is no longer needed. REDUCE is written in COMPASS assembly language.

HELIOS status: The code is operational on CDC 6600 and CDC 7600 computers. Its evolution is still in progress.

Developer/Sponsor:

C. N. Vittitoe
F. Biggs
R. E. Lighthill
Theoretical Division 5231
Sandia Laboratories
Alb., New Mexico 87115

Central Receiver
Systems Branch
Div. of Solar Energy
Energy Research and Dev.
Administration
Washington, D.C. 20545

Documentation: C. N. Vittitoe, F. Biggs, and R. E. Lighthill, HELIOS: A Computer Program for Modeling the Solar Thermal Test Facility, A Users Guide, Sandia

Laboratories Report SAND-76-0346, March 1977, Second edition June 1977.

F. Biggs and C. N. Vittitoe, A Computational Model for Solar Concentrators, Sandia Laboratories Report SAND-76-0347, to be published.

Availability: HELIOS is available from the developers after the potential user obtains approval by the sponsor.

Date: HELIOS became operational in April 1976. The present version of the code was formed in August 1977.

REFERENCES

1. C. N. Vittitoe, F. Biggs, R. E. Lighthill, SAND-76-0346, HELIOS: A Computer Program for Modeling the Solar Thermal Test Facility. A Users Guide, June 1967.

2. F. Biggs and C. N. Vittitoe, SAND-76-0347, A Computational Model for Solar Concentrators, to be published.

3. E. A. Igel, G. F. Bott, R. L. Hughes, Sandia Laboratories Internal Memorandum, April 1977.